

# **Effects of Rigid Segments on Structure and Properties of Unoriented and Oriented Poly(*p*-Phenylene Terephthalamide-co-Ethylene Terephthalates)**

KENJI YAMADA, KAZUTO HASHIMOTO, and MOTOWO TAKAYANAGI, *Department of Applied Chemistry, Faculty of Engineering, Kyushu University, Fukuoka 812, Japan*, YOSHIFUMI MURATA, *Kuraray Co., Ltd., Kurashiki 710, Japan*

## **Synopsis**

In poly(*p*-phenylene terephthalamide-co-ethylene terephthalate) the rigid segments of *p*-phenylene terephthalamide are aggregated as crystalline domains above the weight fraction of the rigid segments, 6 wt%. The rigid segments disturb the crystallization of the flexible segments of poly(ethylene terephthalate) (PET) and are preferentially contained in the amorphous phase of the PET segments. The crystallinity of the PET segments decreased with increasing the content of the rigid segments in the copolymers and the glass transition temperature is decreased by the decrease of the crystallinity below the weight fraction of the rigid segments, 6 wt%, in spite of the depression of micro-Brownian motion of the PET segments due to the rigid segments. The values of Young's modulus  $E$ , yield stress  $\sigma_y$ , and breaking stress  $\sigma_b$  for the zone-drawn copolymer were conspicuously increased by the rigid segments contained in it, in comparison with those of the zone-drawn PET homopolymer. Such higher values of  $E$ ,  $\sigma_y$ , and  $\sigma_b$  of the copolymer are originated by greater increases in the orientation of amorphous chains in the copolymer. The rigid segments in the amorphous phase effectively depressed the thermal shrinkage of the zone-drawn and the zone-annealed copolymers.

## **INTRODUCTION**

Poly(*p*-phenylene terephthalamide) (PPTA) is a rigid polymer which cannot be folded according to the conformational energy calculation.<sup>1</sup> PPTA molecules in the crystalline phases show strong intermolecular interaction owing to the close packing of benzene rings and the strong hydrogen bonding.<sup>1,2</sup> Thus PPTA fiber prepared from a liquid crystalline state in sulfuric acid solution has high modulus and strength.

In this work, the random copolymer, that is, poly(ethylene terephthalate) (PET) containing the rigid segments of *p*-phenylene terephthalamide (PTA) is synthesized to improve the mechanical and thermal properties of PET. In the copolymer strong interaction between the PTA segments would be expected. The oriented copolymers and the oriented PET homopolymers are prepared by means of zone-drawing and zone-annealing methods. The effects of the rigid segments on structure and mechanical and thermal properties of the copolymers are investigated in their unoriented and oriented states.

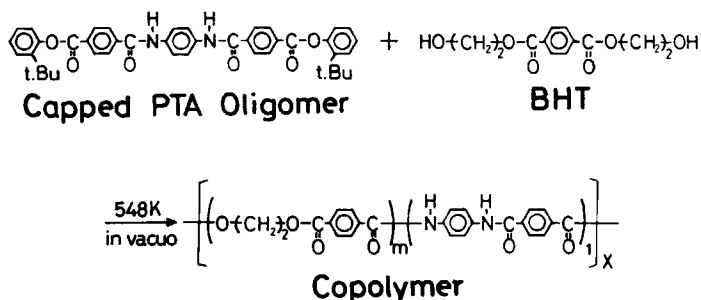


Fig. 1. Scheme of the synthesizing process for poly(*p*-phenylene terephthalamide-*co*-ethylene terephthalate).

## EXPERIMENTAL

### Synthesis of Poly(*p*-Phenylene Terephthalamide-*co*-Ethylene Terephthalate) and the Preparation of its Molded Film

Figure 1 shows the scheme of the synthesizing process for poly(*p*-phenylene terephthalamide-*co*-ethylene terephthalate). Capped PTA oligomers were synthesized according to the procedure proposed previously.<sup>3</sup> The cohesive force of the capped PTA oligomers is depressed by the bulky *o*-tert-butyl phenol. The random copolymers were prepared by polycondensation of *bis* (2-hydroxy ethyl)terephthalate (BHT) with the capped PTA oligomer at 548 K in vacuo (below 0.5 mmHg) for 2 h. The weight fractions of the capped PTA oligomer to BHT monomer were 0/100, 3/97, 6/94, and 9/91, of which the samples are termed hereafter PET homopolymer, 3 wt% PTA/PET, 6 wt% PTA/PET, and 9 wt% PTA/PET copolymers, respectively. In these weight fractions the melt-polycondensation progressed homogeneously. However, the polycondensation did not progress homogeneously at the weight percent of PTA, 20 wt%. The characterization of the copolymers was conducted by proton nuclear magnetic resonance (NMR). The signal of tert-butyl disappeared in the products, and therefore, it becomes apparent that all the PTA segments are introduced into the products by the polycondensation.

The polymerized bulk samples were melt-pressed at 563 K for 5 min and then plunged into ice water to obtain quenched films. The quenched films were annealed at 473 K for 1 h in nitrogen atmosphere to obtain annealed films.

### Preparation of the Oriented Copolymers

The quenched films of the PET homopolymer and the 3 wt% PTA/PET copolymer were uniaxially drawn by using the zone-drawing apparatus equipped with pre- and postquenching zones, as shown in Figure 2.<sup>4-6</sup> The zone-drawn sample was annealed with the same zone-drawing apparatus to prepare a zone-annealed sample. Draw ratio was controlled by changing both the drawing speed and the shifting speed of the ensemble of heater and cooler. The heater temperature was 353 K for zone-drawing and 473 K for zone-

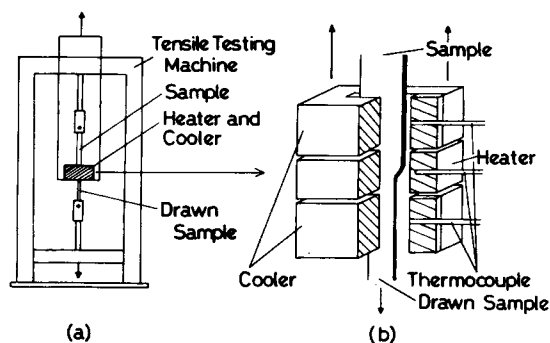


Fig. 2. (a) Schematic representation of forced quenching type zone-drawing and zone-annealing apparatus and (b) the detailed construction of heater and cooler as a part of it.

annealing. The upper cooler temperature was 263 K and the lower was 243 K. A portion of the sample located just above the heater was cooled by using the upper cooler before it was zone-drawn, and therefore the thermal conduction from the heater to the portion was depressed below the glass transition temperature of the sample. The draw ratio was 3.6 for zone-drawing and 4.7 for zone-drawing and then zone-annealing.

### Measurements of Structure and Properties

**Polarizing microscopic observation.** The copolymers were observed in a molten state at 560 K under cross nicols by using a POH polarizing microscope (Nippon Kogaku Co., Ltd.) equipped with hot stage. The birefringences of the zone-drawn and the zone-annealed samples were measured at room temperature with the same microscope.

**X-ray diffraction.** Wide-angle X-ray diffraction (WAXD) photographs of the copolymers were taken with a RU-200 Rotaflex X-ray generator (Rigaku Denki Co., Ltd.). The orientation function of the crystal  $c$  axis of PET was evaluated from the azimuthal intensity distributions of X-ray diffraction from (010), ( $\bar{1}10$ ), and (100) planes by the usual method.

**Differential Scanning Calorimetry (DSC) measurements.** Glass transition temperature ( $T_g$ ), melting temperature ( $T_m$ ), initiation temperature of crystallization ( $T_c$ ), and crystallinity were measured in nitrogen atmosphere with a Unix differential scanning calorimeter (DSC) (Rigaku Denki Co., Ltd.). Heating rate was 10 K/min to measure  $T_g$ ,  $T_m$ , and crystallinity. The copolymers were cooled at 10 K/min from 563 K at which they were held for 5 min, to measure  $T_c$ .

**Density.** Density was measured at 303 K by a flotation method, using  $n$ -heptane-tetrachloromethane mixture.

**Measurements of tensile properties and dynamic viscoelasticity.** The quenched films were uniaxially extended at an initial strain rate of 30%/min at room temperature with a Tensilon UTM-III tensile tester (Toyo Baldwin Co., Ltd.). The zone-drawn samples and the zone-annealed samples were uniaxially extended along the orientation axis at an initial strain rate of

25%/min at room temperature with the same tester. The temperature dependences of dynamic viscoelasticity for the annealed films were measured at 11 Hz in nitrogen atmosphere with a Rheovibron DDV-IIC dynamic viscoelastometer (Toyo Baldwin Co., Ltd.).

**Infrared IR measurement.** Infrared (IR) spectrum was measured at room temperature with a FT/IR-3 Fourier transform infrared spectroscopy (Nippon Bunko Co., Ltd.).

**Thermal shrinkage.** Thermal shrinkage was measured with a Rheovibron DDV-IIC dynamic viscoelastometer (Toyo Baldwin Co., Ltd.) at a heating rate of ca. 3 K/min. The thermal shrinkage is scaled by a parameter of  $(L_0 - L)/L_0 \times 100\%$ , where  $L_0$  is the original length of the sample at room temperature and  $L$  is the value at elevated temperature.

## RESULTS AND DISCUSSION

### Molecular Aggregation State in the Unoriented Copolymers

Figure 3 shows the polarizing micrographs under cross nicols in a molten state at 560 K for (a) the 6 wt% and (b) the 9 wt% PTA/PET copolymers. In the copolymers anisotropic domains were observed, whereas the PET homopolymer and the 3 wt% PTA/PET copolymer were optically isotropic. The polarizing micrographs after quenching the samples were almost the same as in the molten state. Since the anisotropic domains are already observed in the molten state, they would be composed of PTA segments. The number and size of the domains in the 9 wt% PTA/PET copolymer were larger than those in the 6 wt% PTA/PET copolymer. This means that possibility of the formation of PTA aggregates increases with the content of PTA segments. It should be noted that in the 6 wt% and 9 wt% PTA/PET copolymers a certain amount of PTA segments would not be contained in the anisotropic domains but in the amorphous phase of PET.

The above aggregation states of PTA segments are confirmed by the WAXD photographs of the quenched films. Figure 4 shows WAXD photographs of the quenched films of the PET homopolymer and the copolymers. In the PET homopolymer, amorphous halo was observed, but Debye rings were not done. This result means that the amorphous state in the molten state of the PET homopolymer would be frozen effectively by the quenching process and the crystalline phases are not formed. In the 6 wt% PTA/PET copolymer only a Debye ring of Bragg spacing,  $d = 0.435$  nm was observed with amorphous halo, whereas in the 3 wt% PTA/PET copolymer no Debye rings were observed and only amorphous halo was done. In the 9 wt% PTA/PET copolymer three Debye rings were observed with amorphous halo. The Bragg spacings of these Debye rings were 0.521 nm, 0.435 nm, and 0.394 nm, of which the values are almost coincident with the plane distances of (010), (110), and (200) in the crystalline structure of poly(*p*-phenylene terephthalamide),<sup>2</sup> and therefore the Debye rings would have originated from the crystalline aggregates composed of PTA segments.

From the WAXD photographs of the annealed films of the PET and copolymers, it becomes apparent that PET molecules are crystallized by annealing at 473 K for 1 h.

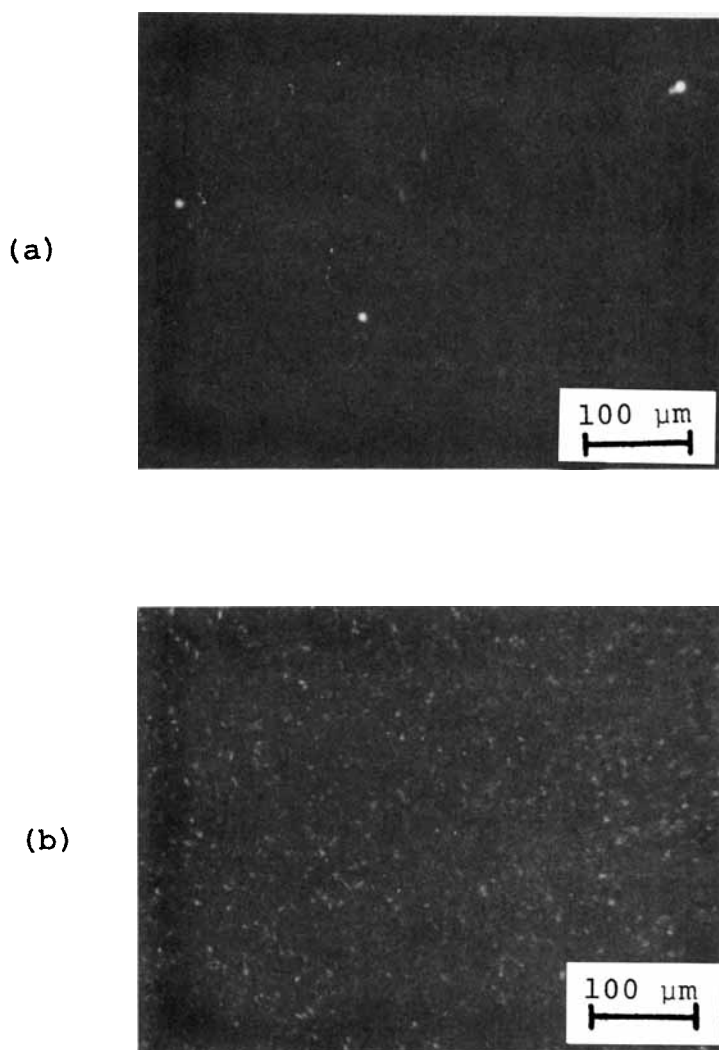


Fig. 3. Polarizing micrographs under cross nicols in a molten state at 560 K for (a) the 6 wt% PTA/PET and (b) the 9 wt% PTA/PET copolymers.

#### Effects of PTA Segments on Thermal and Mechanical Properties in the Unoriented Copolymers

Figure 5 shows a change in glass transition temperature  $T_g$  with increasing PTA content in the quenched films.  $T_g$  increased with increasing PTA content and the  $T_g$  curve was concave. This result suggests that the PTA segments in the copolymer would effectively restrain the micro-Brownian motion of PET segments.

The relationship between a melting temperature  $T_m$  and the molar fraction of PET segments  $X_A$  is shown for the annealed films in Figure 6. The solid line in the figure was drawn by assuming the following proportional relation-

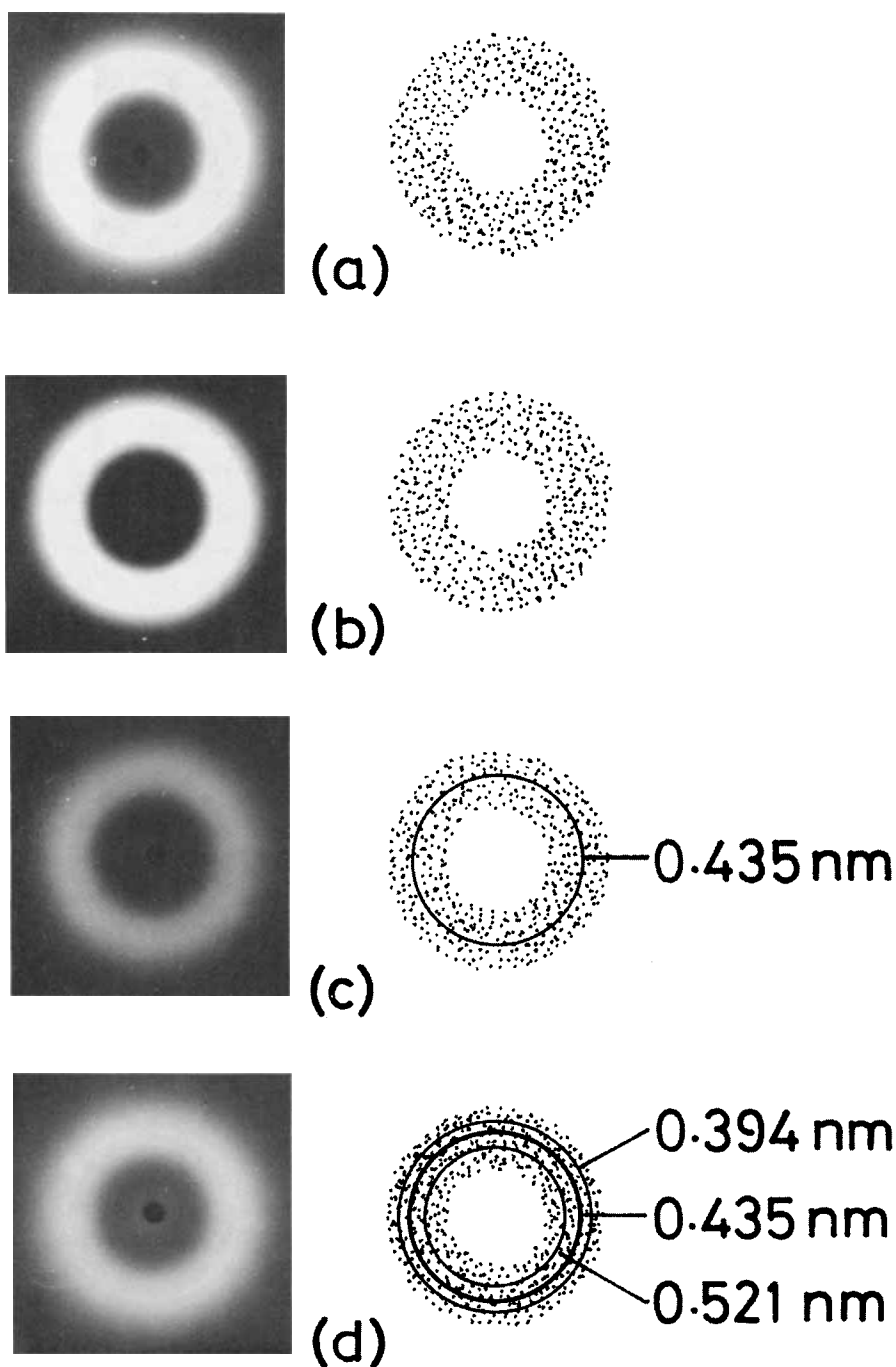


Fig. 4. Wide-angle X-ray diffraction photographs of the quenched films; (a) the PET homopolymer, (b) the 3 wt% PTA/PET, (c) the 6 wt% PTA/PET, and (d) the 9 wt% PTA/PET copolymers.

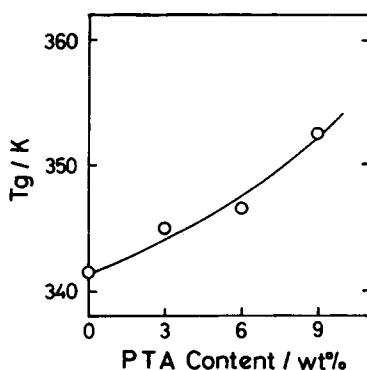


Fig. 5. Glass transition temperature  $T_g$  as a function of PTA content in the quenched films.

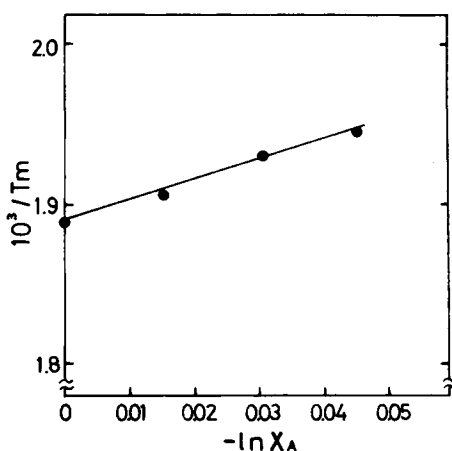


Fig. 6.  $1/T_m$  as a function of  $-\ln X_A$  for the annealed films.

ship:

$$1/T_m \propto -\ln X_A$$

This relationship coincides qualitatively with Flory's equation.<sup>7</sup> It may be assumed that the growth of PET crystals along the molecular axis is disturbed by PTA segments and thus the PTA segments do not enter in the PET crystalline phase. In the 6 wt% and 9 wt% PTA/PET copolymers, a certain amount of PTA segments form in the crystalline domains, as shown in Figures 3 and 4.

Figure 7 shows the crystallinity of PET segments as a function of PTA content for the annealed films. The crystallinity was evaluated from the area of the endothermic peak in melting. In this case, the value of 121 J/g<sup>8</sup> was used as the heat of fusion for the crystalline phase of PET. Crystallinity decreased monotonically with increasing PTA content. Crystallinity evaluated from density also decreased with increasing PTA content. The decrease in the crystallinity means that PTA segments disturb the crystallization of PET segments and are preferentially contained in the amorphous phase of PET

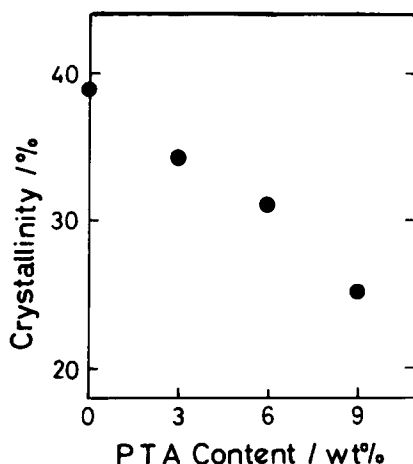


Fig. 7. Crystallinity as a function of PTA content for the annealed films.

segments. The beginning temperatures  $T_c$ 's of the crystallization from the molten state of the copolymers were lower than that of the PET homopolymer. Below the PTA content of 6 wt%,  $T_c$  decreased with increasing PTA content, but the  $T_c$  for the 9 wt% PTA/PET copolymer was scarcely different from that of the 6 wt% PTA/PET copolymer. The decrease of  $T_c$  would be originated by the PTA segments which restrain the molecular motion of PET segments necessary to the crystallization, whereas the PTA aggregates formed in the molten state of the copolymer may act as nuclei for the crystallization of PET segments and accelerate the crystallization rate of PET segments to result in the increase of  $T_c$ . The formation of the PTA aggregates in the molten state of the copolymers was shown in Figure 3. The depression of the molecular motion of PET segments by the PTA segments may preferentially take place below the PTA content of 6 wt%, but the acceleration of the crystallization rate of PET segments by the PTA aggregates may largely occur at the PTA content of 9 wt%, in addition to the depression of the PET molecular motion by the PTA segments.

Figure 8 shows the temperature dependence of storage modulus  $E'$  and loss modulus  $E''$  at 11 Hz for the annealed films. The  $E''$  peaks around the temperatures of 390 K to 400 K are associated with the micro-Brownian motion of amorphous chains for the PET homopolymer and the copolymers. The  $E''$  peak temperatures in the copolymers were around 400 K, independent of the fraction of PTA segments, and were higher than the temperature in the PET, ca. 390 K. The glass transition temperature  $T_g$  in the annealed film depends on the following factors: (1) crystallinity  $\chi$  of PET segments and (2) the fraction of the PTA segments contained in the amorphous region. Since the  $T_g$  decreases with decreasing  $\chi$ <sup>9</sup> and  $\chi$  decreases with increasing PTA content (Fig. 7), the  $T_g$  should decrease with increasing PTA content. The increase of PTA content in the amorphous phase brings about the increase of  $T_g$ , taking into account the increase of  $T_g$  with PTA content in the quenched film (Fig. 5). Therefore, the PTA segments are more effective with increased  $T_g$ , compared with the negative effect due to decreased crystallinity.



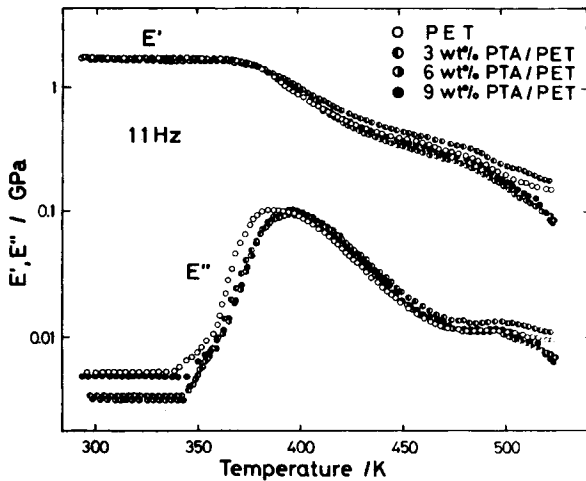


Fig. 8. Temperature dependence of storage modulus  $E'$  and loss modulus  $E''$  at 11 Hz for the annealed films.

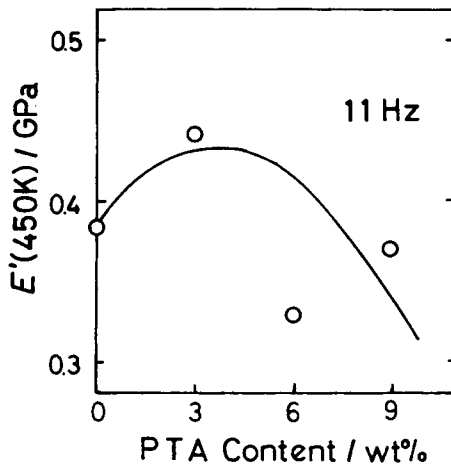


Fig. 9. Storage modulus  $E'$  at 11 Hz at 450 K as a function of PTA content for the annealed films.

The values of  $E'$  in the copolymers were almost the same as that of the PET homopolymer below the glass transition temperature. Above the  $T_g$ , the decrease of  $E'$  in the 3 wt% PTA/PET copolymer became smaller than that of the PET, whereas  $E'$  in the 6 wt% and 9 wt% PTA copolymers decreased more than that in the PET. Figure 9 shows the values of  $E'$  at 450 K as a function of PTA content for the annealed films. It can be assumed that the value of  $E'$  above the  $T_g$  decreases with decreasing crystallinity, but increases with increasing content of PTA segments contained in the amorphous phase. That is to say, the effects of the crystallinity and the PTA content on  $E'$  are compensated by each other. Therefore, it becomes apparent that in the 3 wt% PTA/PET copolymer the PTA segments contained in the amorphous phase are more effective on the increase of  $E'$ , compared with the negative effect of

crystallinity. On the other hand, in the 6 wt% and 9 wt% PTA/PET copolymers crystallinity is more effective with the decrease of  $E'$ .

According to the results of tensile tests for the quenched films, both Young's moduli and yield stresses in all the copolymers below the PTA content of 9 wt% were almost the same as those of the PET homopolymer, whereas the breaking stress and the strain at breaking decreased with increasing PTA content. The following section will examine how the tensile properties of the copolymers are much improved by zone-drawing and zone-annealing, compared with those of the PET homopolymer.

### Effects of PTA Segments on Structure and Properties of the Oriented Copolymers

Table I shows birefringence  $\Delta n$ , orientation function  $f_c$  of  $c$  axis in PET crystalline phase, orientation function  $f_a$  of amorphous chains, and volume crystallinity  $\chi_v$  of PET segments for the zone-drawn (Z-D) samples and the zone-annealed (Z-A) samples. These samples are the PET homopolymers and the 3 wt% PTA/PET copolymers. The value of  $f_a$  was evaluated by using the values of  $\Delta n$ ,  $f_c$ , and  $\chi_v$  as follows:

$$f_a = \frac{\Delta n - \chi_v f_c \Delta_c^0}{(1 - \chi_v) \Delta_a^0}$$

where  $\Delta_c^0$  and  $\Delta_a^0$  are the intrinsic birefringences in the PET crystalline phase and amorphous phase, respectively. The values of  $\Delta_c^0$  and  $\Delta_a^0$  are 0.220<sup>10</sup> and 0.295,<sup>10</sup> respectively, and the effect of PTA segments on the intrinsic birefringence of the amorphous phase was neglected. Both the  $f_c$  and  $f_a$  of the Z-A samples were higher than those of the Z-D samples. There were almost no differences in  $f_c$  between the PTA/PET copolymers and the PET homopolymers, whereas  $f_a$ 's of the PTA/PET copolymers were much higher than those of the PET homopolymers. From wide-angle X-ray diffraction photographs of the Z-D and Z-A samples, the spacings evaluated from the diffractions of the crystalline phase of the PTA/PET copolymers agreed with those of the PET homopolymers. These results suggest that the PTA segments in the copolymer selectively exist in the PET amorphous phase and raise the orientation of PET amorphous chains through the interaction between the PTA and PET segments.

TABLE I  
Birefringence  $\Delta n$ , orientation function of  $c$  axis in PET crystalline phase  $f_c$ , orientation function of amorphous chains  $f_a$ , and volume crystallinity  $\chi_v$  for the zone-drawn samples and the zone-annealed samples

Sample	$\Delta n$	$f_c$	$f_a$	$\chi_v/\%$
Z-D PET	0.130	0.964	0.376	24.4
Z-D 3 wt% PTA/PET	0.156	0.961	0.497	25.9
Z-A PET	0.174	0.993	0.393	59.7
Z-A 3 wt% PTA/PET	0.191	0.991	0.552	59.2

TABLE II  
Absorbance ratios A973/A1042 of  $973\text{ cm}^{-1}$  to  $1042\text{ cm}^{-1}$   
for the zone-drawn samples and the zone-annealed samples

Sample	A973/A1042
Z-D PET	1.55
Z-D 3 wt% PTA/PET	1.90
Z-A PET	2.70
Z-A 3 wt% PTA/PET	3.02

The fractional ratio of *trans* to gauche conformation in the PET segments contained in the amorphous phase would be qualitatively compared between the PET homopolymer and the copolymer by using IR spectra. The IR bands associated with the *trans* and gauche conformations are  $973\text{ cm}^{-1}$  and  $1042\text{ cm}^{-1}$ , respectively.<sup>11</sup> From the absorbances of the bands, A973 and A1042, the ratios A973/A1042 are obtained in Table II. The values of the ratios in the Z-A samples are higher than those in the Z-D samples, since the conformation of PET segments in the crystalline phase is *trans* and the crystallinity of the Z-A sample is higher than that of the Z-D sample. In cases both of zone-drawing and zone-annealing, the values of the ratio in the 3 wt% PTA/PET copolymers are always higher than those in the PET homopolymers, even if in both the Z-D and Z-A samples the crystallinity of the 3 wt% PTA/PET copolymer is almost the same as that of the PET homopolymer (Table I). This result means that the fractions of *trans* conformation in the amorphous phases of the 3 wt% PTA/PET copolymers are higher than those of the PET homopolymers. Therefore, the increase of orientation function of amorphous chains in the copolymer is originated by the increase of the *trans* conformation of the PET segments contained in the amorphous phase.

Figures 10(a) and 10(b) show stress-strain curves of the Z-D and Z-A samples which are the PET homopolymers and the 3 wt% PTA/PET copo-

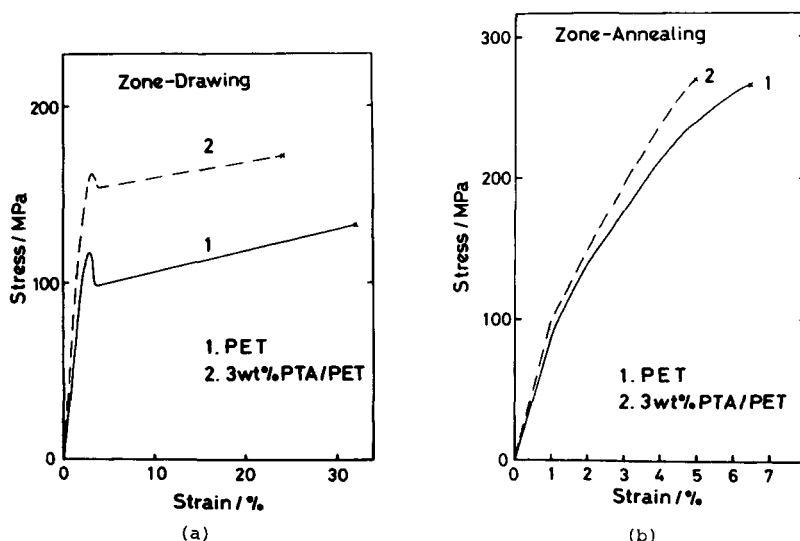


Fig. 10. Stress-strain curves at room temperature for (a) the zone-drawn samples and (b) the zone-annealed samples.

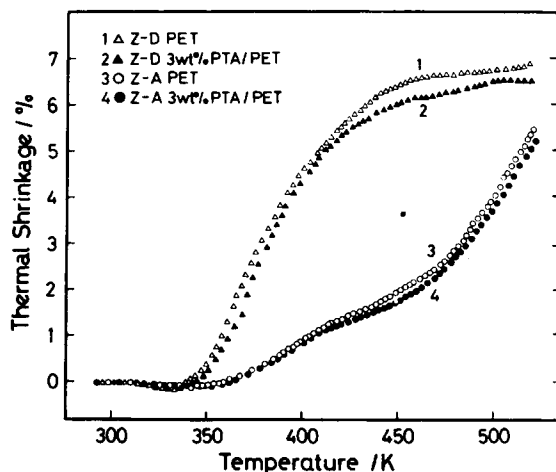


Fig. 11. Thermal shrinkage curves at the heating rate of ca. 3 K/min for the zone-drawn samples and the zone-annealed samples.

lymers. The Young's modulus  $E$ , the yield stress  $\sigma_y$ , and the breaking stress  $\sigma_b$  for the Z-D copolymer were conspicuously increased by the PTA segments contained in it, in comparison with those of the Z-D PET homopolymer. The  $E$  of the Z-A copolymer was also increased by the PTA segments. Such higher values of  $E$ ,  $\sigma_y$ , and  $\sigma_b$  of the copolymer originated with greater increases in the orientation of amorphous chains in the copolymer (Table I).

Figure 11 shows thermal shrinkage curves at the heating rate of ca. 3 K/min for the Z-D and Z-A samples. In both the Z-D and Z-A samples the amount of thermal shrinkage of the copolymer was slightly depressed in comparison with that of the PET homopolymer at the same temperatures. In the zone-drawn polypropylene the higher the orientation function of amorphous chains, the larger was the thermal shrinkage.<sup>12</sup> The orientation function of amorphous chains in the 3 wt% PTA/PET copolymer was always higher than that in the PET homopolymer (Table I). Therefore, the result of Figure 11 suggests that PTA segments in the amorphous phase effectively depressed the thermal shrinkage of the copolymer owing to the strong interaction between the PTA segments and their high rigidity. Thus, it becomes apparent from Figures 10 and 11 that PTA segments in the uniaxially oriented samples are effective in the improvement of the mechanical properties and depression of the thermal shrinkage.

## CONCLUSION

In poly(*p*-phenylene terephthalamide-co-ethylene terephthalate) the rigid segments of *p*-phenylene terephthalamide (PTA) are aggregated as crystalline domains above the weight fraction of the rigid segments, 6 wt%. PTA segments are preferentially contained in the amorphous phase of the flexible segments of poly(ethylene terephthalate) (PET) and would effectively restrain the micro-Brownian motion of PET segments. The crystallinity of the PET segments decreased with increasing content of rigid segments. PTA segments are effective in higher values of storage modulus  $E'$  above the glass transition

temperature.

The values of Young's modulus  $E$ , yield stress  $\sigma_y$ , and breaking stress  $\sigma_b$  for the zone-drawn copolymer were conspicuously increased by the rigid segments, in comparison with those of the zone-drawn PET homopolymer. Such higher values of  $E$ ,  $\sigma_y$ , and  $\sigma_b$  are originated by a greater increase in the orientation of amorphous chains. The increase of the *trans* conformation of the PET segments contained in the amorphous phase is originated by the rigid segments and results in the increase of orientation function of the amorphous chains. The rigid segments in the amorphous phase effectively depressed the thermal shrinkage of the zone-drawn and the zone-annealed copolymers.

### References

1. K. Tashiro, M. Kobayashi, and H. Tadokoro, *Macromolecules*, **10**, 413 (1977).
2. M. G. Northolt and J. J. van Aartsen, *J. Polym. Sci., B*, **11**, 333 (1973).
3. Kuraray Co., Ltd., Japan Kokai Tokkyo Koho, 82-137321.
4. M. Kamezawa, K. Yamada, and M. Takayanagi, *J. Appl. Polym. Sci.*, **24**, 1227 (1979).
5. K. Yamada and M. Takayanagi, *J. Appl. Polym. Sci.*, **27**, 2091 (1982).
6. K. Yamada, M. Oie, and M. Takayanagi, *J. Polym. Sci. Polym. Phys. Ed.*, **27**, 1063 (1983).
7. P. J. Flory, *Trans. Faraday Soc.*, **51**, 848 (1955).
8. R. C. Roberts, *Polymer*, **10**, 113 (1969).
9. K. H. Illers and H. Breuer, *J. Colloid Sci.*, **18**, 1 (1963).
10. J. H. Dumbleton, *J. Polym. Sci., A-2*, **6**, 795 (1968).
11. A. Miyake, *J. Polym. Sci.*, **38**, 479 (1959).
12. K. Yamada, M. Kamezawa, and M. Takayanagi, *J. Appl. Polym. Sci.*, **26**, 49 (1981).

Received January 27, 1986

Accepted June 5, 1986